

Landmark-based Prostate MR Image Matching Using Incompressible Large Deformation Diffeomorphism

X. Liu¹, S. Roys², J. L. Prince^{1,3}, and R. Gullapalli²

¹Computer Science, Johns Hopkins University, Baltimore, MD, United States, ²Radiology, University of Maryland Baltimore, Baltimore, MD, United States, ³Electrical and Computer Engineering, Johns Hopkins University, Baltimore, MD, United States

Introduction: Magnetic resonance (MR) imaging with an endorectal coil is a standard clinical procedure for prostate cancer diagnosis. The balloon used with the endorectal coil is typically inflated to as high as 100 cc for optimal coupling of the coil with the prostate gland, and minimizing movement of the gland during the image or spectral acquisition. However, this method of acquisition deforms the prostate from its native state while images and spectra are obtained. For optimum delivery of radiation dose to the areas of cancer, the information obtained in the deformed state needs to be transformed back to its native state. Registration methods that have been proposed to date [1,2] are either rigid or non-rigid and compressible, neither of which accounts for the true nature of the prostate deformation [3]. In this work we constrained the deformation field to be incompressible, and developed an incompressible landmark-based image matching method using the large deformation diffeomorphism (LDD) framework [4], and applied it to transform the deformed prostate to its native state.

Methods: Our method matches manually specified landmarks on the deformed and non-deformed prostate images using large deformation diffeomorphism (LDD) framework. Given N landmark pairs $((x_n, y_n), n = 1, \dots, N)$, the LDD finds a diffeomorphism $\phi(x, t)$ that maps any point x in the source image to its position y in the target image such that $t \in [0, 1]$ and $\phi(x, 0) = x$, $\phi(x, 1) = y$. The velocity field $v(x, t)$ at time t is defined as the time derivative of $\phi(x, t)$. Unlike the small deformation interpolation, the LDD does not constrain directly the displacement field. Instead, it computes the velocity fields that minimizes the quadratic energy function $E(v) = \iint_{\Omega_t} \|Lv(x, t)\|^2 dx dt$ and satisfies $\phi(x_n, 1) = y_n$, $n = 1, \dots, N$, where L is a differential operator. The deformation field is finally computed by integrating v over t . In addition, the velocity field of an incompressible object is divergence free everywhere. A vector spline solution was previously proposed [5] to interpolate a divergence-free vector field. The vector spline minimizes the energy function $J(v) = \int \|\nabla \text{curl}(v(x))\|^2 dx$ with the constraint $\text{div}(v(x)) = 0$, where $\text{div}(\cdot)$ and $\text{curl}(\cdot)$ are the vector divergence and curl respectively. It has been shown that the kernel matrix of this differential operator is $K(x) = \{-\Delta + \nabla \nabla^T\}h(\|x\|)$, where $h(r) = r^4 \log r$ for two dimensions and $h(r) = r^3$ for three dimensions. By incorporating the divergence-free vector spline into the LDD framework we reformulated the problem as: finding the velocity field $\hat{v}(x, t) = \arg \min_v \iint_{\Omega_t} \|\nabla \text{curl}(v(x, t))\|^2 dx dt$ that satisfies $\text{div}(v(x)) = 0$ and $\phi(x_n, 1) = y_n$, $n = 1, \dots, N$. The velocity $\hat{v}(x, t)$ and the mapping $\phi(x, t)$ are then solved using discrete time points and iterative gradient descent [4]. We call this the *incompressible LDD* method.

Results: Figure 1 demonstrates the method using a numerical example that has 2 matching points and 4 fixed corner points, as shown in Fig. 1a. In Figs. 1a & d, points A and B move to C and D respectively. Figs. 1a-c show the results of standard LDD, and Figs. 1d-f are the results of the proposed incompressible LDD method respectively. In (a) and (d), the red lines show the trajectories of points using the two different methods. Fig. 1b & e shows the final deformation using deformed grids. Fig. 1c & f are the vector flow of the displacement fields. It is clear that the grid areas are not preserved in the standard LDD solution, while they are preserved in the incompressible LDD solution. The incompressibility of the mesh produces a vortex in the displacement field (shown in Fig. 1f).

We also applied our incompressible LDD method on three T2-weighted prostate datasets (3mm slice thickness, TE/TR 80/3000ms) to transform the deformed prostate images to their native state. For each dataset one image volume was acquired with the coil inserted but with no air in the balloon (Fig. 2a), while the other was acquired when the balloon was inflated with 60cc air. These images were then matched using small deformation registration (thin-plate spline), standard LDD, and incompressible LDD methods, and the results were compared. Fig. 2 shows the results on one of the datasets. The red crosses mark the landmark points chosen. In Fig 2, (a) is the non-deformed image, (b) shows the deformation computed using standard LDD, while (c) shows results of incompressible LDD. We also computed the determinants of Jacobian of the motion field, which is shown in Fig. 3. Figs. 3a-c are the results of incompressible LDD, standard LDD, and thin-plate spline interpolation respectively. The determinant of the Jacobian indicates the local volume change. For an incompressible object, its value remains 1 everywhere. From Fig. 3 we can see the deformation produced by incompressible LDD retains this property, while in the standard LDD and the small deformation registration, the volume change can be as high as 30%.

Conclusion: In this work we developed a landmark-based prostate MR image registration method using incompressible large deformation diffeomorphism. By enforcing the divergence-free condition on the velocity fields the final deformation field is a true reflection of the physical property of prostate. Although the current implementation of this method is limited to 2D images, an extension to 3D is currently under development. In the future we will also include the application of incompressible LDD method to motion estimation and interpolation of incompressible moving tissues, for example, the heart and the tongue.

Acknowledgement: This work is supported by NIH grant R01 HL047405 and grant from DOD Award No. W81XWH-04-1-0249.

References:

1. Fei B, et al., *Comput. Med. Imag.*, 27:267-281, 2003
2. Venugopal N, et al., *Phys. Med. Biol.*, 50:2871-2885, 2005
3. Krouskop TA, et al., *Ultrasound Imag.*, 20:260-274, 1998
4. Joshi SC, et al., *IEEE Trans. Imag. Proc.*, 9(8):1357-1370, 2000
5. Amodei L, et al., *Journ. Approx. Theo.*, 67(1):51-79, 1991

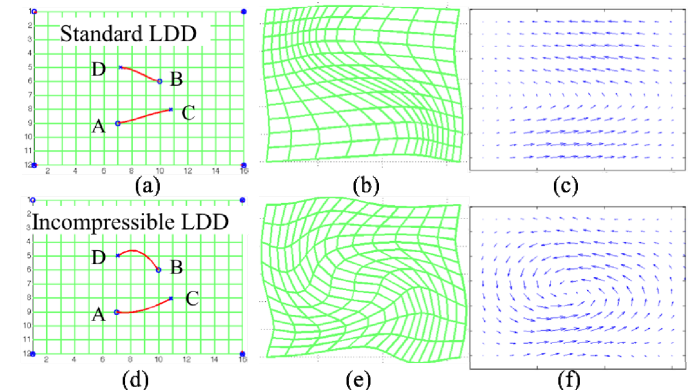


Fig. 1 Numerical example

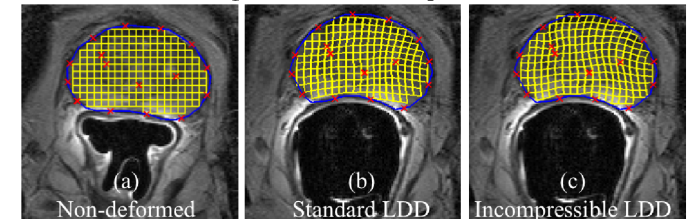


Fig. 2 Results on prostate image matching

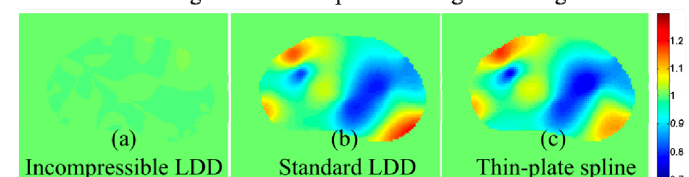


Fig. 3 Determinant of Jacobian of deformation field